A General Framework for Mixed-Domain Echo Cancellation in Discrete Multitone Systems

Neda Ehtiati and Benoît Champagne

***Abstract*—In full-duplex communication systems with discrete multi-tone (DMT) modulation, echo cancellers are employed to cancel echo by means of adaptive filters. Generally, the structure present in the DMT signals is used to decrease the computational complexity of these cancellers by splitting the operations between the time and frequency domains. In this work, we introduce a general framework for designing echo cancellers for such systems in an arbitrary mixed domain. This is achieved by introducing a generic decomposition of the Toeplitz data matrix at the transmitter in terms of arbitrary unitary matrices. Then, based on this decomposition, a new mixed-domain echo cancellation structure is derived, which performs an exact instantaneous gradient-type adaptation. This mixed-domain configuration is also extended for realizing constrained adaptation whereby linear constraints are used to ensure the proper mapping of the weight vectors in different domains. The proposed structures offer a unified framework to study existing cancellers and to design new ones with better performance measures. This framework is employed to propose a new canceller based on discrete trigonometric transformations. The analytical and numerical results presented show that this canceller has a faster convergence rate than the existing ones with similar complexity and is more robust.**

***Index Terms*—Echo cancellation, discrete multitone modulation, transform domain adaptive filters, DSL systems.**

I. Introduction

In DSL systems, the upstream and downstream signals are sent over a single twisted-pair of copper wires, using a hybrid circuit. Ideally, signals should travel from the line into the receiver and from the transmitter into the line, without interfering on each other. However, there is always leakage of signals from the transmitter into the collocated receiver, which is known as electrical echo. In full-duplex DSL systems, various duplexing techniques, such as frequency-division duplexing (FDD), digital duplexing and echo cancellation, can be used to separate the upstream and downstream signals [1].

In FDD, a frequency gap separates the bands used for the upstream and downstream transmission, using precise analog filters with sharp transition characteristics. In recent DSL standards which accommodate various frequency band plans, the use of fixed filters is prohibitive; instead, digital duplexing is employed, where the signals in the two directions are kept orthogonal to each other by adding cyclic suffixes (CS) [2]. However, this technique is applicable only to the short loops with lengths under 1 km [3], [4]. In systems with echo cancellation (EC), digital adaptive filters are used to estimate the echo and remove it from the transmitted signal [5]. The benefits of using digital echo cancellers are multiple: the requirements on the front-end filters can be relaxed; the need for a frequency gap between the downstream and upstream is removed, resulting in a higher spectral efficiency; finally, for systems with digital duplexing, the use of echo canceller makes the service available on longer loops.

The results in [6] show that under similar operating conditions (i.e., bandwidth and SNR margin), the maximum achievable downstream bit-rate for the FDD-ADSL is lower by 7% compared to that of EC-ADSL. Alternatively, for achieving a similar downstream rate as EC-ADSL, FDD-ADSL requires 30% more bandwidth, or its maximum achievable distance must be reduced by 10%. These improvements in EC-ADSL are achieved at the expense of additional computational complexity for performing the signal processing and result in increased dynamic range at the input of the receiver. In the case of VDSL technologies, for VDSL1 the physical reach is limited to around 1500m on 0.4mm cable, whereas the reach of VDSL2 is around 2400m [4]. The digital duplexing method, used in VDSL1, can only compensate for delay effects on the loops shorter than 1km. Therefore, in VDLS2 systems for medium and long loop applications, ITU-T G.933.2 standard deploys the use of echo cancellers and time-domain equalizers to reach the required performance [7].

In DSL systems using DMT modulation, the time-domain echo cancellation involves the multiplication of the emulated echo channel response by a Toeplitz data matrix containing the transmitted signal samples (thereby performing the linear convolution). To avoid this costly matrix multiplication, the Toeplitz data matrix is usually decomposed into a sum of simpler components that allows the calculations to be performed in different domains with reduced complexity. Consequently, various mixed time- and frequency-domain echo cancellers have beed proposed in the literature, e.g., the circular echo synthesis canceller [8], [9], the circulant decomposition canceller [10] and the symmetric decomposition canceller [11].

These cancellers reduce the complexity by performing the echo emulation partially in the time and frequency domains, while an approximate per-tone weight update is done entirely in the frequency domain. However, not all the tones are always used (excited) in DMT-based systems, because of

Paper approved by C.-L.Wang, the Editor for Equalization of the IEEE Communications Society. Manuscript received April 29, 2011; revised January 19, April 25, and July 4, 2012.

The authors are with the Department of Electrical and Computer Engineering, McGill University, 3480 University St., Montréal, H3A 2A7 Canada (e-mail: neda.ehtiati@mail.mcgill.ca, benoit.champagne@mcgill.ca).

Funding for this work was provided in part by a grant from the Natural Sciences and Engineering Research Council of Canada. Part of this work has been presented at the IEEE GLOBECOM 2009 Conference and IEEE ICASSP Conference 2010.

Authors would like to thank the anonymous reviewers for their constructive comments that help improve the quality of this manuscript.

Digital Object Identifier 10.1109/TCOMM.2012.120512.110258

certain power masks requirements or due to the bit allocation algorithm. As a result, these methods, especially the CES canceller [9], may suffer from slow convergence caused by the lack of sufficient excitation on the unused tones during the weight update step. To improve the convergence, transmission of dummy data with reduced power on the unused tones is proposed [12]. However, this generates extra interference, demanding a more complex equalization, and also requires higher-order front end filters to comply with the power masks [13]. The cancellers proposed in [10], [11] are less effected by the lack of excitation, since the tap-input vector used for the weight update in these algorithms usually has sufficient excitation on all tones.

The study of the aforementioned echo cancellers reveals that they share a common design methodology, whereby a means of decomposing the Toeplitz data matrix is first chosen, and then the adaptive canceller is developed from this choice. This approach has the disadvantage that the choice of the employed decomposition imposes some limitations on the canceller which directly affect its performance, e.g., sensitivity to lack of excitation on the unused tones in cancellers employing frequency domain operations. The choice of the decomposition explicitly defines matrix transformations being used and the domains in which the echo emulation and adaptive update are performed. Therefore, this decision has a direct impact on the complexity and the convergence of the algorithm.

In this work, we propose to modify the order of echo canceller design methodology. In our proposed approach, a novel generic decomposition of the Toeplitz data matrix in terms of arbitrary unitary matrices is introduced. These unitary matrices are used to define generic domains for performing echo emulation and adaptive weight update, using the transformed weight vectors and time-domain signals. Consequently, a new mixed-domain canceller (MDC) structure is proposed, where an exact least mean square (LMS) adaptive filtering can be performed in the transform domain. The proposed strategy has the advantage that the structure of the echo canceller can be optimized towards achieving better convergence rate and/or lower complexity without having any limitations imposed by the choice of the decomposition. In [14], we showed that the mixed time- and frequency-domain echo cancellation methods can be viewed as a linearly constrained optimization and we developed a new canceller which incorporates linear constraints. In addition, it was shown that *a priori* knowledge about the echo channel can often be translated into linear constraints, which can be used as well to improve the performance of the canceller. Accordingly, in this work, we propose a constrained MDC (CMDC), where linear constraints are applied in a general mixed domain to ensure the proper mapping of the weight vectors in different domains.

The proposed mixed-domain structure offers a unified representation of existing echo cancellers, where these methods correspond to specific, approximate cases of this general form. More importantly, this new framework provides significant design flexibility in achieving a proper trade-off between convergence rate and computational complexity in the echo cancellation algorithms. This capability can be realized by using various decompositions of the Toeplitz data matrix in the MDC and CMDC structures. In the final part of this work, we examine the criteria for an appropriate decomposition to be used in the implementation of the proposed mixed-domain structures, in the sense of reducing the computational complexity. We propose a specific implementation which utilizes the discrete trigonometric transformations in a combined form of MDC and CMDC structures, referred to as mixed trigonometric canceller (MTC). The analytical convergence proof and the simulated results provided show that the MTC has similar complexity to the existing echo cancellation methods but with faster convergence rate and also is not sensitive to the lack of excitation on the unused tones.

The rest of this paper is structured as follows. In Section II, current methods for echo cancellation for DMT-based systems are reviewed. In Section III, the general decomposition of the Toeplitz data matrix and MDC framework are introduced. In Section IV, CMDC structure is presented, and the convergence in the mean for these mixed-domain structures are examined in Section V. The implementation of these structures in the form of MTC algorithm is discussed in Section VI. Finally, in Section VII, the simulation results providing the learning curves for the proposed and the existing echo cancellers are given. The following notations are used: The square identity matrix of size N is denoted by $\mathcal{I}_N$, and the all-zero matrix of size $N \times M$ is denoted by $\mathbf{0}_{N\times M}$. The discrete Fourier transformation and its inverse are denoted by $\mathcal{F}_N$ and $\mathcal{F}_N^{-1}$, respectively. Finally, $\mathrm{diag}\{\mathbf{v}\}$ indicates a diagonal matrix whose diagonal elements are given by vector $\mathbf{v}$, and $\odot$ denotes component-wise multiplication.

II. Background

In this paper, for convenience we assume symmetric data rates at the transceiver where the modulation and demodulation are performed by the use of IDFT/DFT of equal length N. The transmitted time-domain symbol at symbol period k, is $\mathbf{u}^k = [u_0^k, \cdots, u_{N-1}^k]^T$, where u_i^k $(i = 0, \cdots, N-1)$ represents the i^{th} time-domain sample obtained from the N-point IDFT of the vector containing the QAM modulated data in the frequency domain [1]. The emulated echo $\mathbf{y}_e^k$ at symbol period k is generated by the linear convolution of the transmitted symbols and the weight vector of the adaptive filter, $\mathbf{w}^k$, modeling the echo channel at that time. This can be expressed as

$$\mathbf{y}_e^k = \mathcal{U}^k \bar{\mathbf{M}} \mathbf{w}^k, \tag{1}$$

where matrices $\mathcal{U}^k$ and $\bar{\mathbf{M}}$ are defined as follows. In the general asynchronous case, there is a misalignment or delay of Δ samples between the echo frames and received far-end frames. Therefore, matrix $\mathcal{U}^k$ in (1), is an $N \times N$ Toeplitz matrix consisting of elements from symbols, $\mathbf{u}^{k-1}$, $\mathbf{u}^k$ and $\mathbf{u}^{k+1}$: its first row is given by $[u_\Delta^k, \cdots, u_0^k, u_{N-1}^k, \cdots, u_{N-\upsilon}^k, u_{N-1}^{k-1}, \cdots, u_{\Delta+\upsilon+1}^{k-1}]$ and its first column is $[u_\Delta^k, \cdots, u_{N-1}^k, u_{N-\upsilon}^{k+1}, \cdots, u_{N-1}^{k+1}, u_0^{k+1}, \cdots, u_{\Delta-\upsilon-1}^{k+1}]^T$, where υ is the length of the cyclic prefix. The weight vector $\mathbf{w}^k$ of length T_e, in (1), represents the estimate of the true echo channel impulse response, which models the effects of the hybrid circuit, the digital and analog front end filters and the time-domain equalizer. The $N \times T_e$ matrix $\bar{\mathbf{M}} \triangleq [\mathcal{I}_{T_e} | \mathcal{O}_{T_e\times(N-T_e)}]^T$ is used to pad $\mathbf{w}^k$ with zeros.

The emulated echo is then subtracted from the received symbol $\mathbf{y}^k$, resulting in the error signal

$$\mathbf{e}^k = \mathbf{y}^k - \mathbf{y}_e^k. \tag{2}$$

Consequently, the echo weights can be obtained adaptively using various methods, e.g., the LMS algorithm, in which the error signal is used to update the weights iteratively [5].

To avoid the costly matrix multiplication in (1), Ho *et al.* introduced the circular echo synthesis (CES) canceller, in [9], where the matrix $\mathcal{U}^k$ is decomposed as a sum:

$$\mathcal{U}^k = \mathcal{X}^k + \mathcal{L}^k \tag{3}$$

where $\mathcal{L}^k$ is a circulant matrix with first column given by $[u_\Delta^k, \cdots, u_{N-1}^k, u_0^k, \cdots, u_{\Delta-1}^k]^T$ and $\mathcal{X}^k = \mathcal{U}^k - \mathcal{L}^k$ is a residual component [1]. The circulant matrix $\mathcal{L}^k$ can now be diagonalized using the DFT and IDFT matrices, $\mathcal{L}^k = \mathcal{F}_N^{-1}\,\mathrm{diag}\{\mathbf{\Lambda}^k\}\,\mathcal{F}_N$, where the elements of $\mathbf{\Lambda}^k$ are obtained as the Fourier transform of the first column of $\mathcal{L}^k$. Furthermore, the error signal transformed into the frequency domain (i.e., $\mathbf{E}^k = \mathcal{F}_N\,\mathbf{e}^k$) can be written as

$$\mathbf{E}^k = \mathcal{F}_N(\mathbf{y}^k - \mathcal{X}^k\,\bar{\mathbf{M}}\,\mathbf{w}^k) - \mathbf{\Lambda}^k \odot \mathbf{W}^k \tag{4}$$

where $\mathbf{W}^k = \mathcal{F}_N\,\bar{\mathbf{M}}\,\mathbf{w}^k$ is the Fourier transform of the zero-padded weights. The error signal is then used to update the echo weights, where the diagonalization in the frequency domain allows a per-tone *approximate* LMS update, given by

$$\mathbf{W}^{k+1} = \mathbf{W}^k + \mu\,(\mathbf{\Lambda}^k)^* \odot \mathbf{E}^k, \tag{5}$$

with μ denoting the step-size. As discussed earlier, since not all the tones are excited in the frequency domain, this method suffers from poor convergence, unless dummy data with reduced power are transmitted on the unused tones.

To ameliorate the convergence of the CES echo canceller, Ysebaert *et al.* proposed the circulant decomposition canceller (CDC) in [10], where the Toeplitz matrix $\mathcal{U}^k$ is decomposed into a sum of circulant and skew-circulant matrices, i.e.,

$$\mathcal{U}^k = \frac{1}{2}\overbrace{(\mathcal{U}^k + \mathcal{S}^k)}^{\text{circulant part}} + \frac{1}{2}\overbrace{(\mathcal{U}^k - \mathcal{S}^k)}^{\text{skew-circulant part}} \tag{6}$$

where the $N \times N$ matrix $\mathcal{S}^k$ is defined such that the $2N \times 2N$ matrix $\tilde{\mathcal{L}}^k \triangleq \begin{bmatrix} \mathcal{U}^k & \mathcal{S}^k \\ \mathcal{S}^k & \mathcal{U}^k \end{bmatrix}$ is circulant. The circulant matrix $\tilde{\mathcal{L}}^k$ can be similarly diagonalized, with diagonal elements $\tilde{\mathbf{\Lambda}}^k$ obtained from the Fourier transform of the first column of $\tilde{\mathcal{L}}^k$. Based on the diagonalization of $\tilde{\mathcal{L}}^k$, the matrix $\mathcal{U}^k$ in (6) can be written as (for more details see [13])

$$\mathcal{U}^k = \frac{1}{2}\,\mathcal{F}_N^{-1}\,\mathrm{diag}\{\tilde{\mathbf{\Lambda}}_{\text{even}}^k\}\,\mathcal{F}_N + \frac{1}{2}\,\mathbf{Q}^H\,\mathcal{F}_N^{-1}\,\mathrm{diag}\{\tilde{\mathbf{\Lambda}}_{\text{odd}}^k\}\,\mathcal{F}_N\,\mathbf{Q} \tag{7}$$

where $\tilde{\mathbf{\Lambda}}_{\text{even}}^k$ and $\tilde{\mathbf{\Lambda}}_{\text{odd}}^k$ are obtained from the even and odd numbered elements of $\tilde{\mathbf{\Lambda}}^k$, respectively, and $\mathbf{Q} = \mathrm{diag}\{[1, e^{-j\pi/N}, \cdots, e^{-j\pi(N-1)/N}]^T\}$.

Consequently, the transformed error signal is now given by

$$\mathbf{E}^k = \mathcal{F}_N\left(\mathbf{y}^k - \frac{1}{2}\mathbf{Q}^H\,\mathcal{F}_N^{-1}\,(\tilde{\mathbf{\Lambda}}_{\text{odd}}^k \odot \tilde{\mathbf{W}}^k)\right) - \frac{1}{2}\tilde{\mathbf{\Lambda}}_{\text{even}}^k \odot \mathbf{W}^k \tag{8}$$

[1]In [9], the CES canceller is formulated for a synchronous case where $\Delta = 0$; here, we consider a more general asynchronous case as in [13].

where $\mathbf{W}^k$ is the weight vector in the frequency domain, and $\tilde{\mathbf{W}}^k = \mathcal{F}_N\,\mathbf{Q}\,\bar{\mathbf{M}}\,\mathbf{w}^k$. The per-tone approximate weight update is performed similarly to (5) in the frequency domain as

$$\mathbf{W}^{k+1} = \mathbf{W}^k + \mu\,(\tilde{\mathbf{\Lambda}}_{\text{even}}^k)^* \odot \mathbf{E}^k, \tag{9}$$

and $\tilde{\mathbf{W}}^{k+1} = \mathcal{F}_N\,\mathbf{Q}\,\bar{\mathbf{M}}\,\bar{\mathbf{M}}^T\,\mathcal{F}_N^{-1}\,\mathbf{W}^{k+1}$, which can be performed infrequently every ψ iterations. As shown in [10], if $\Delta \neq -\upsilon$, then the CDC algorithm provides an acceptable convergence since the elements of $\tilde{\mathbf{V}}_{\text{even}}^k$ are nonzero.

In [11], Pisoni and Bonaventura propose a symmetric decomposition canceller (SDC) where the Toeplitz matrix $\mathcal{U}^k$ is decomposed using discrete cosine and sine transforms (DCT and DST). The symmetric decomposition is based on [15], where it is shown that the trigonometric transformers can be utilized to diagonalize a Toeplitz matrix written as a combination of specific Toeplitz and Hankel matrices. Therefore, the original Toeplitz matrix $\mathcal{U}^k$ is rewritten as follows

$$\begin{aligned}\mathcal{U}^k = {} & \frac{1}{4}(\mathcal{T}_S^k + \mathcal{H}_S^k) + \frac{1}{4}(\mathcal{T}_S^k - \mathcal{H}_S^k) \\ & - \frac{1}{4}(\mathcal{T}_A^k + \mathcal{H}_A^k) - \frac{1}{4}(\mathcal{T}_A^k - \mathcal{H}_A^k).\end{aligned} \tag{10}$$

where $\mathcal{T}_S^k$ is a symmetric Toeplitz matrix with its first row given by the vector $\mathbf{a}^k$, with entries $a^k(i) = \mathcal{U}^k(0,i) + \{\mathcal{U}^k(i,0)\}^*$ for $i = 0, \cdots, N-1$, and $\mathcal{T}_A^k$ is an anti-symmetric Toeplitz matrix with its first row given by the vector $\mathbf{b}^k$, with entries $b^k(i) = \mathcal{U}^k(0,i) - \{\mathcal{U}^k(i,0)\}^*$ for $i = 0, \cdots, N-1$. In addition, $\mathcal{H}_S^k$ is a persymmetric Hankel matrix with its first row given as $[a^k(i), \cdots, a^k(N-1), 0]$ and $\mathcal{H}_A^k$ is an anti-persymmetric Hankel matrix with first row $[b^k(1), \cdots, b^k(N-1), 0]$.

Using the DCT and DST, each term in (10) can be individually diagonalized, yielding

$$\begin{aligned}\mathcal{U}^k = {} & (\mathcal{C}^{\text{II}})^T\,\tilde{\mathcal{Z}}^T\mathcal{D}^k\,\tilde{\mathcal{Z}}\mathcal{C}^{\text{II}} + (\mathcal{S}^{\text{II}})^T\,\mathcal{Z}^T\mathcal{D}^k\,\mathcal{Z}\mathcal{S}^{\text{II}} \\ & + (\mathcal{C}^{\text{II}})^T\,\tilde{\mathcal{Z}}^T\tilde{\mathcal{D}}^k\,\mathcal{Z}\mathcal{S}^{\text{II}} - (\mathcal{S}^{\text{II}})^T\,\mathcal{Z}^T\tilde{\mathcal{D}}^k\,\tilde{\mathcal{Z}}\mathcal{C}^{\text{II}}\end{aligned} \tag{11}$$

where $\mathcal{C}^{\text{II}}$ and $\mathcal{S}^{\text{II}}$ are $N \times N$ DCT-II and DST-II matrices, respectively [16], and the $(N+1) \times N$ matrices $\mathcal{Z} = [\mathbf{0}_{N\times 1}|\mathcal{I}_N]^T$ and $\tilde{\mathcal{Z}} = [\mathcal{I}_N|\mathbf{0}_{N\times 1}]^T$ are shift matrices. The $(N+1) \times (N+1)$ matrices $\mathcal{D}^k = \frac{1}{2}\mathrm{diag}\{\mathbf{d}^k\}$ and $\tilde{\mathcal{D}}^k = \frac{1}{2}\mathrm{diag}\{[0, (\tilde{\mathbf{d}}^k)^T, 0]^T\}$, where the vectors $\mathbf{d}^k = \tilde{\mathcal{C}}^{\text{I}}\,[a^k(0), \cdots, a^k(N-1), 0]^T$ and $\tilde{\mathbf{d}}^k = \tilde{\mathcal{S}}^{\text{I}}\,[b^k(1), \cdots, b^k(N-1)]^T$ are resulted from the transformation by the non-normalized $(N+1)\times(N+1)$ DCT-I matrix $\tilde{\mathcal{C}}^{\text{I}}$ and $(N-1) \times (N-1)$ DST-I matrix $\tilde{\mathcal{S}}^{\text{I}}$ [16], respectively.

In this method, the echo emulation is performed using the decomposition in (11). For updating the weights, the connection between the CDC and SDC methods is derived, where the vector $\tilde{\mathbf{\Lambda}}_{\text{even}}^k$ is calculated directly from the SDC elements and (9) is employed to update the weights in the frequency domain. Therefore, both algorithms have similar convergence, since they use the same weight update formula.

III. General Mixed-Domain Echo Cancellation

As discussed earlier, the choice of the decomposition applied to Toeplitz data matrix $\mathcal{U}^k$ has a direct impact on the performance of the echo cancellers. In this section, we first introduce a general form of decomposition of the matrix $\mathcal{U}^k$

and show that various representations used in the existing echo cancellers comply with this general form. Next, based on this general decomposition, we develop a general mixed-domain canceller (MDC) which performs the adaptive weight update and echo emulation in the generic transform domains. This approach enables us to further analyze and simplify the echo canceller structure, regardless of the decomposition used.

A. General decomposition of Toeplitz data matrix

In general, the Toeplitz data matrix $\mathcal{U}^k$ can be decomposed in a mixed transform domain as follows

$$\mathcal{U}^k = [\mathcal{G}_1^H \quad \mathcal{G}_2^H] \begin{bmatrix} \mathcal{S}_{11}^k & \mathcal{S}_{12}^k \\ \mathcal{S}_{21}^k & \mathcal{S}_{22}^k \end{bmatrix} \begin{bmatrix} \mathcal{G}_1 \\ \mathcal{G}_2 \end{bmatrix} \tag{12}$$

where $\mathcal{G}_i$ $(i = 1, 2)$ are $N \times N$ unitary matrices which are constant for all symbol periods, and $\mathcal{S}_{i,j}^k$ $(i, j = 1, 2)$ are $N \times N$ matrices, with their elements calculated based on the transmitted symbols. This general form provides a proper structure to incorporate the decompositions used in the existing echo cancellers, as shown below.

In the CES canceller presented by Ho *et al.* in [9], the matrix $\mathcal{U}^k$ is decomposed as presented in (3). It can be seen that this decomposition is a special case of the general form (12) with:

$$\mathcal{U}^k = [\mathcal{F}_N^{-1} \quad \mathcal{I}_N] \begin{bmatrix} \text{diag}\{\mathbf{\Lambda}^k\} & \mathcal{O}_N \\ \mathcal{O}_N & \mathcal{X}^k \end{bmatrix} \begin{bmatrix} \mathcal{F}_N \\ \mathcal{I}_N \end{bmatrix} \tag{13}$$

where the vector $\mathbf{\Lambda}^k$ and the matrix $\mathcal{X}^k$ are defined as in the previous section, and the matrices $\mathcal{G}_1 = \mathcal{F}_N$ and $\mathcal{G}_2 = \mathcal{I}_N$.

The decomposition of the matrix $\mathcal{U}^k$ used in the CDC algorithm [10] is given in (7). Similarly, expressed in the general format, the decomposition of the matrix $\mathcal{U}^k$ can be rewritten as

$$\mathcal{U}^k = \left[\mathcal{F}_N^{-1} \quad \mathbf{Q}^H \mathcal{F}_N^{-1}\right] \cdot \begin{bmatrix} \frac{1}{2}\text{diag}\{\tilde{\mathbf{\Lambda}}_{\text{even}}^k\} & \mathcal{O}_N \\ \mathcal{O}_N & \frac{1}{2}\text{diag}\{\tilde{\mathbf{\Lambda}}_{\text{odd}}^k\} \end{bmatrix} \begin{bmatrix} \mathcal{F}_N \\ \mathcal{F}_N \mathbf{Q} \end{bmatrix} \tag{14}$$

where the vectors $\tilde{\mathbf{\Lambda}}_{\text{even}}^k$ and $\tilde{\mathbf{\Lambda}}_{\text{odd}}^k$ and the matrix $\mathbf{Q}$ are as defined earlier, and $\mathcal{G}_1 = \mathcal{F}_N$ and $\mathcal{G}_2 = \mathcal{F}_N \mathbf{Q}$.

Finally, the symmetric decomposition used in the SDC algorithm [11], given in (11), can be expressed as

$$\mathcal{U}^k = \left[(\mathcal{C}^{\text{II}})^T \quad (\mathcal{S}^{\text{II}})^T\right] \begin{bmatrix} \tilde{\mathcal{Z}}^T \mathcal{D}^k \tilde{\mathcal{Z}} & \tilde{\mathcal{Z}}^T \tilde{\mathcal{D}}^k \mathcal{Z} \\ -\mathcal{Z}^T \tilde{\mathcal{D}}^k \tilde{\mathcal{Z}} & \mathcal{Z}^T \mathcal{D}^k \mathcal{Z} \end{bmatrix} \begin{bmatrix} \mathcal{C}^{\text{II}} \\ \mathcal{S}^{\text{II}} \end{bmatrix} \tag{15}$$

where the involved matrices $\mathcal{D}^k$, $\tilde{\mathcal{D}}^k$, $\mathcal{Z}$ and $\tilde{\mathcal{Z}}$ have been introduced previously, and $\mathcal{G}_1 = \mathcal{C}^{\text{II}}$ and $\mathcal{G}_2 = \mathcal{S}^{\text{II}}$ are the DCT-II and DST-II, respectively [16]. In this decomposition, the corresponding submatrices $\mathcal{S}_{11}^k$ and $\mathcal{S}_{22}^k$ are diagonal. It can also easily be verified that the submatrix $\mathcal{S}_{12}^k$ has non-zero elements only on the super-diagonal and the submatrix $\mathcal{S}_{21}^k$ has non-zero elements only on the sub-diagonal.

As shown above, the general decomposition in (12) provides a unified representation for the previously used decompositions of the matrix $\mathcal{U}^k$[2]. In the rest of this paper, the short form of the decomposition in (12) is used, as denoted by

$$\mathcal{U}^k = \mathcal{G}^H \mathcal{S}^k \mathcal{G}, \tag{16}$$

where the $2N \times N$ matrix $\mathcal{G}$ and the $2N \times 2N$ matrix $\mathcal{S}^k$ are defined as:

$$\mathcal{G} \triangleq \begin{bmatrix} \mathcal{G}_1 \\ \mathcal{G}_2 \end{bmatrix}, \quad \mathcal{S}^k \triangleq \begin{bmatrix} \mathcal{S}_{11}^k & \mathcal{S}_{12}^k \\ \mathcal{S}_{21}^k & \mathcal{S}_{22}^k \end{bmatrix}. \tag{17}$$

In the following section, we utilize this general form to propose a general mixed-domain echo canceller structure.

B. Mixed-domain canceller

Using the generic decomposition of the matrix $\mathcal{U}^k$ in (16), the emulated echo in the time domain, given in (1), can be rewritten as

$$\mathbf{y}_e^k = \mathcal{G}^H \mathcal{S}^k \mathcal{G} \mathbf{M} \mathbf{w}^k, \tag{18}$$

where the $2N \times T_e$ matrix $\mathbf{M} \triangleq [\frac{\bar{\mathbf{M}}}{\mathbf{M}}]$. The decomposition (12) implicitly defines the available physical domains (e.g., time, frequency, etc.) for performing the calculations, via the choice of the submatrices of $\mathcal{G}$, i.e., $\mathcal{G}_1$ and $\mathcal{G}_2$.

Therefore, the emulated echo can be mapped into the mixed transform domain, using the matrix $\mathcal{G}$, i.e.,

$$\mathbf{Y}_e^k \triangleq \mathcal{G} \mathbf{y}_e^k = \mathcal{G} \mathcal{G}^H \mathcal{S}^k \mathcal{G} \mathbf{M} \mathbf{w}^k. \tag{19}$$

Based on (19), the transformed input data matrix is defined as

$$\mathbf{\Phi}^k \triangleq (\mathcal{S}^k)^H \mathcal{G} \mathcal{G}^H, \tag{20}$$

and the mapped weight vector into the transform domain using $\mathcal{G}$ is expressed by

$$\boldsymbol{\omega}^k \triangleq \mathcal{G} \mathbf{M} \mathbf{w}^k. \tag{21}$$

Therefore, the estimated echo in the transform domain is $\mathbf{Y}_e^k = (\mathbf{\Phi}^k)^H \boldsymbol{\omega}^k$.

To use adaptive methods, e.g., LMS algorithm, for updating the weight vector, the error signal must be calculated. In the transform domain, the error signal vector is obtained by

$$\mathbf{E}^k = \mathbf{Y}^k - (\mathbf{\Phi}^k)^H \boldsymbol{\omega}^k \tag{22}$$

where $\mathbf{Y}^k = \mathcal{G} \mathbf{y}^k$ is the transformed received signal. Using the LMS algorithm, the echo weights are updated by

$$\boldsymbol{\omega}^{k+1} = \boldsymbol{\omega}^k + \mu \mathbf{\Phi}^k \mathbf{E}^k. \tag{23}$$

Equations (22) and (23) jointly describe an adaptive mixed-domain echo canceller, where (23) performs an adaptation of the weight vector using the LMS weight update.

In the existing echo cancellers, the mixed-domain calculations are partially used in the echo emulation step but replaced by an approximate per-tone frequency-domain weight update to reduce the complexity. The use of this approximation deteriorates the convergence of the adaptive algorithms and in some cancellers, e.g., CES canceller, makes it sensitive to the lack of excitation on the unused tones.

The adaptive update in (23) is computationally costly because of the calculation involved for determining the matrix $\mathbf{\Phi}^k$; however, as shown below and as in [18], a computationally efficient equivalent weight update can be derived.

Substituting the value of $\mathbf{\Phi}^k$ from (20) and using the definition of the error signal in (22), the adaptive update in

[2]It should be noted that the general decomposition of the matrix $\mathcal{U}^k$ was first proposed by authors in [17].

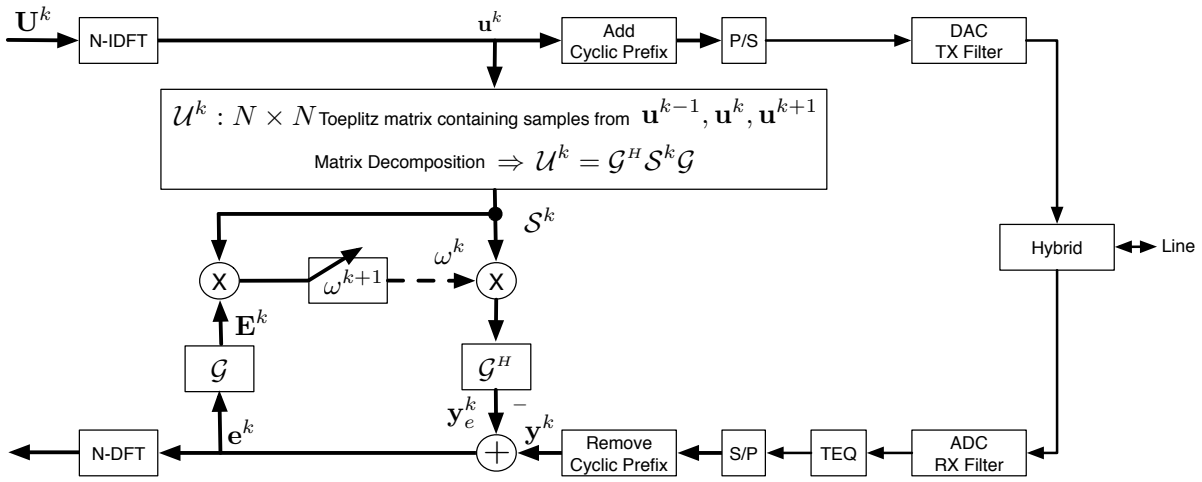

Fig. 1: Block diagram of the mixed-domain canceller (MDC).

(23) can be rewritten as

$$\boldsymbol{\omega}^{k+1} = \boldsymbol{\omega}^k + \mu\,(\mathcal{S}^k)^H\,\mathcal{G}\,\mathcal{G}^H\,\left(\mathcal{G}\,\mathbf{y}^k - \mathcal{G}\,\mathcal{G}^H\,\mathcal{S}^k\,\boldsymbol{\omega}^k\right) \quad (24)$$

Since, the submatrices of $\mathcal{G}$ are unitary matrices, $\mathcal{G}^H\mathcal{G} = 2\mathcal{I}_N$. Therefore, the weight update can be written as

$$\begin{aligned}\boldsymbol{\omega}^{k+1} &= \boldsymbol{\omega}^k + \mu\,(\mathcal{S}^k)^H\mathcal{G}\,\left(\mathbf{y}^k - \mathcal{G}^H\,\mathcal{S}^k\,\boldsymbol{\omega}^k\right)\\ &= \boldsymbol{\omega}^k + \mu\,(\mathcal{S}^k)^H\mathbf{E}^k. \end{aligned} \quad (25)$$

where the factor 2 is incorporated in μ. Equations (22) and (25) jointly describe an adaptive algorithm which we refer to as the mixed-domain canceller (MDC). The block diagram for this structure is shown in Fig. 1. In this canceller, the estimated echo is calculated in the transform domain yet subtracted from the received signal in the time domain, to avoid the calculations of the matrix $\mathbf{\Phi}^k$ in the emulation step. Then, the error signal is mapped into the transform domain, and the weights are updated in the transform domain entirely by (25). In Section VI, we show that the simplified structure of MDC can be used in conjunction with an appropriate decomposition to design new echo cancellers with reduced complexity.

IV. Linearly Constrained Mixed-Domain Echo Cancellation

In [14], we introduced a linearly constrained echo cancellation framework, where linear constraints on the time- and frequency-domain weight vectors can be applied to improve the performance of the canceller. Consequently, two constrained cancellers had been developed: one based on the work by Frost in [19] and the second one based on the generalized sidelobe canceller (GSC) structure by Griffiths and Jim in [20]. In this section, a more generalized form of these linearly constrained echo cancellers is developed, where the weight vectors and signals are presented in mixed transform domain. We also examine a specific formulation of this constrained canceller where the corresponding constraint matrix ensures the proper relation between the weight vectors in the mixed domains.

A. Linearly constrained echo cancellation in mixed domain

In [14], we showed that the echo cancellation problem can be formulated as a constrained optimization where the appropriate cost function, expressed as the mean-square of the error signal vector, is minimized under constraints. Therefore, considering the error vector for the MDC structure in the mixed domain, as given by (22), the echo canceller design can be described by the following constrained optimization:

$$\min_{\boldsymbol{\omega}^k} \mathrm{E}[\|\mathbf{E}^k\|^2] \quad \text{s.t. } \mathcal{C}^H\,\boldsymbol{\omega}^k = \mathbf{g}. \quad (26)$$

In (26), $\boldsymbol{\omega}^k$ is the weight vector in the transform domain, the $(2N) \times l_c$ matrix $\mathcal{C}$ is the full-column rank constraint matrix and the vector $\mathbf{g}$ is of length l_c, where l_c is the number of constraints and $l_c < 2N$[3].

Linearly constrained echo cancellers had been derived based on approaches by Frost [19] and Griffiths and Jim [20] in [14]. Using similar methods, we can develop linearly constrained canceller for the MDC structure[4]. For this constrained canceller, the adaptive weight update based on the Frost approach in the mixed domain is given by

$$\boldsymbol{\omega}^{k+1} = \boldsymbol{\omega}_q + \mathcal{P}_c^{\perp}\left(\boldsymbol{\omega}^k + \mu\,\mathbf{\Phi}^k\,\mathbf{E}^k\right) \quad (27)$$

where $\boldsymbol{\omega}_q = \mathcal{C}(\mathcal{C}^H\mathcal{C})^{-1}\mathbf{g}$ is the quiescent term, matrix $\mathcal{P}_c^{\perp}$ is the projector onto the orthogonal complement of the subspace spanned by the constraint matrix $\mathcal{C}$, and $\mathcal{P}_c^{\perp} = \mathcal{I}_{2N} - \mathcal{C}(\mathcal{C}^H\mathcal{C})^{-1}\mathcal{C}^H$.

As noted earlier, the main difference between the above canceller and the one developed in [14] is the domains in which the signals are represented. In the former, the weight vectors and signals are expressed in the transform domains defined by the submatrices of $\mathcal{G}$. Therefore, different realizations of this canceller can be obtained by choosing different decompositions of the Toeplitz data matrix in (12).

[3]Since the transformations used are unitary, the squared error in the transform domain is equivalent to the time-domain squared error.

[4]The main focus here is on the constrained MDC structure based on the Frost method, while similar results for the GSC-based canceller can also be easily derived.

B. Constrained mixed-domain canceller

In the mixed domain, the weight vector $\boldsymbol{\omega}^k = \begin{bmatrix} \boldsymbol{\omega}_1^k \\ \boldsymbol{\omega}_2^k \end{bmatrix}$, where the two components result from the transformation of the time-domain weight vector by the corresponding submatrices of $\mathcal{G}$, i.e., $\boldsymbol{\omega}_i^k = \mathcal{G}_i\,\bar{\mathbf{M}}\,\mathbf{w}_i^k$ for $i = 1, 2$. Accordingly, these two components are not independent of each other and the proposed constraint matrix $\mathcal{C}$ in (26) should be defined in a way so as to ensure the proper relationship between these two components. This association can be achieved by forcing the vectors $\boldsymbol{\omega}_1^k$ and $\boldsymbol{\omega}_2^k$ to have equal inverse transformations in the time domain, i.e., $\bar{\mathbf{M}}^T\,\mathcal{G}_1^H\,\boldsymbol{\omega}_1^k = \bar{\mathbf{M}}^T\,\mathcal{G}_2^H\,\boldsymbol{\omega}_2^k$, which yields T_e constraints.

In addition, we can add constraints for the practical case where the length of the FIR filter modeling the echo channel is smaller than the frame size, i.e., $T_e < N$. To this end, the last $N - T_e$ weights of the inverse transformations of $\boldsymbol{\omega}_1^k$ and $\boldsymbol{\omega}_2^k$ into the time domain are forced to zero. Equivalently, using matrix notations, we have: $\tilde{\mathbf{M}}^T\,\mathcal{G}_1^H\,\boldsymbol{\omega}_1^k = \mathcal{O}_{(N-T_e)\times 1}$ and $\tilde{\mathbf{M}}^T\,\mathcal{G}_2^H\,\boldsymbol{\omega}_2^k = \mathcal{O}_{(N-T_e)\times 1}$ where the $N \times (N - T_e)$ matrix $\tilde{\mathbf{M}} \triangleq [\mathcal{O}_{(N-T_e)\times T_e} | \mathcal{I}_{(N-T_e)}]^T$ extracts the last $N - T_e$ weights.

These constraints can be incorporated into a single equation, as in (26), by defining the full-rank constraint matrix $\mathcal{C}$ as follows:

$$\mathcal{C} = \begin{bmatrix} \mathcal{G}_1\tilde{\mathbf{M}} & \mathcal{G}_1\bar{\mathbf{M}} & \mathcal{O}_{N\times N-T_e} \\ \mathcal{O}_{N\times N-T_e} & -\mathcal{G}_2\bar{\mathbf{M}} & \mathcal{G}_2\tilde{\mathbf{M}} \end{bmatrix}. \tag{28}$$

In addition, the gain vector in (26) $\mathbf{g} = \mathcal{O}_{(2N-T_e)\times 1}$.

Using this choice of matrix $\mathcal{C}$, we can develop a constrained mixed-domain canceller (CMDC) based on the Frost LMS approach expressed in (27). It can be easily verified that for this constraint matrix the projection matrix $\mathcal{P}_c^{\perp} = \frac{1}{2}\mathcal{G}\mathbf{M}\mathbf{M}^T\mathcal{G}^H$ and the quiescent term $\boldsymbol{\omega}_q = \mathcal{O}_{2N\times 1}$. By substituting the values for $\mathcal{P}_c^{\perp}$ and $\boldsymbol{\omega}_q$ in (27), the adaptive weight update formula for the CMDC algorithm, for the given constraint matrix, is obtained as

$$\boldsymbol{\omega}^{k+1} = \frac{1}{2}\,\mathcal{G}\mathbf{M}\mathbf{M}^T\mathcal{G}^H\,(\boldsymbol{\omega}^k + \mu\,\boldsymbol{\Phi}^k\,\mathbf{E}^k). \tag{29}$$

Similar arguments as in Section III-B can be used to show that (29) is equivalent to

$$\boldsymbol{\omega}^{k+1} = \frac{1}{2}\,\mathcal{G}\mathbf{M}\mathbf{M}^T\mathcal{G}^H\,(\boldsymbol{\omega}^k + \mu\,(\mathcal{S}^k)^H\mathbf{E}^k). \tag{30}$$

The adaptive weight update in (30) expresses the final version of the proposed CMDC algorithm for the chosen constraint matrix in (28).

V. Convergence Analysis of Mixed-domain Cancellers

A comparison of convergence rates between the proposed MDC and CMDC algorithms and the existing cancellers is possible by means of computer simulations, where the results are given in Section VII. The convergence in the mean of these LMS-based algorithms can also be studied by deriving the recursion for the mean weight-error vector in the mixed domain and identifying the equivalent transformed data correlation matrix, characterizing this recursion. Ultimately, the eigenvalue spread of this matrix determines the convergence rate of the algorithms [5]. Below, the convergence of the MDC and CMDC are examined analytically using this approach.

We make the following assumptions which are generally used in the convergence study of LMS-based algorithms [12], [13]. We assume that the received signal can be modeled as the output of an FIR filter with additive white Gaussian noise, with the noise being uncorrelated to the transmitted echo symbols. In addition, the transmitted echo symbols are uncorrelated with each other and the frequency-domain elements within each symbol are also uncorrelated with each other. This assumption implies that the samples of time-domain vectors from one sample period to the other are independent (excluding the prefix), which is not always valid in practice, but regularly used to prove the convergence of echo cancellers.

To study the convergence of the unconstrained MDC algorithm, the error signal can be substituted from (22) and the adaptive weight update in (25) can be rewritten as

$$\boldsymbol{\omega}^{k+1} = \left(\mathcal{I}_{2N} - \mu\,(\mathcal{S}^k)^H\,\mathcal{G}\,\mathcal{G}^H\,\mathcal{S}^k\right)\boldsymbol{\omega}^k + \mu\,(\mathcal{S}^k)^H\,\mathcal{G}\,\mathbf{y}^k. \tag{31}$$

If the optimal transformed weight vector $\mathbf{H} \triangleq \mathcal{G}\,\mathbf{h}$ is subtracted from both sides of (31), the resulting weight-error vector $\Delta^k \triangleq \boldsymbol{\omega}^k - \mathbf{H}$ is given by

$$\begin{aligned} \Delta^{k+1} &= \left(\mathcal{I}_{2N} - \mu\,(\mathcal{S}^k)^H\,\mathcal{G}\,\mathcal{G}^H\,\mathcal{S}^k\right)\Delta^k \\ &\quad + \mu\,(\mathcal{S}^k)^H\,\mathcal{G}\,\underbrace{\left(\mathbf{y}^k - \mathcal{G}^H\,\mathcal{S}^k\,\mathbf{H}\right)}_{\mathbf{n}^k}. \end{aligned} \tag{32}$$

When taking the expectation on both sides of the equation, the second term is cancelled, since the received noise $\mathbf{n}^k$ and the input data are uncorrelated. Furthermore, since the data vectors are uncorrelated, the expectation of the product of weight-error vector and transformed input data can be separated, resulting in

$$\mathrm{E}[\Delta^{k+1}] = \mathrm{E}[\mathcal{I}_{2N} - \mu\,(\mathcal{S}^k)^H\,\mathcal{G}\,\mathcal{G}^H\,\mathcal{S}^k]\,\mathrm{E}[\Delta^k]. \tag{33}$$

Therefore, the convergence rate for the mean weight-error vector of the unconstrained MDC algorithm is determined by the correlation matrix $\mathcal{R}_{\text{UC}} = \mathrm{E}[(\mathcal{S}^k)^H\,\mathcal{G}\,\mathcal{G}^H\,\mathcal{S}^k]$.

As shown in [19], the correlation matrix corresponding to the constrained LMS algorithm can be derived based on the one of the unconstrained LMS algorithm. Therefore, for the CMDC algorithm, the correlation matrix of the constrained algorithm denoted by $\mathcal{R}_{\text{C}}$ is given by

$$\mathcal{R}_{\text{C}} = \mathcal{P}_c^{\perp}\,\mathcal{R}_{\text{UC}}\,\mathcal{P}_c^{\perp}, \tag{34}$$

where $\mathcal{P}_c^{\perp}$ is the projection matrix and $\mathcal{R}_{\text{UC}}$ is the correlation of the unconstrained algorithm. Based on the general result in [19], it can also be verified that the correlation matrix $\mathcal{R}_{\text{C}}$ has precisely l_c zero eigenvalues, where l_c is the number of constraints. In addition, this correlation matrix has $2N - l_c$ non-zero eigenvalues, which are bounded between the smallest and largest eigenvalues of $\mathcal{R}_{\text{UC}}$.

To simplify the discussion, we focus on the specific case where the length of the echo channel is equal to the frame size, i.e., $T_e = N$. Under this condition, we have $\mathbf{M} = \mathcal{I}_N$ and the projection matrix $\mathcal{P}_c^{\perp} = \frac{1}{2}\mathcal{G}\,\mathcal{G}^H$, representing $l_c = N$ linear constraints. Using these simplifications, the correlation

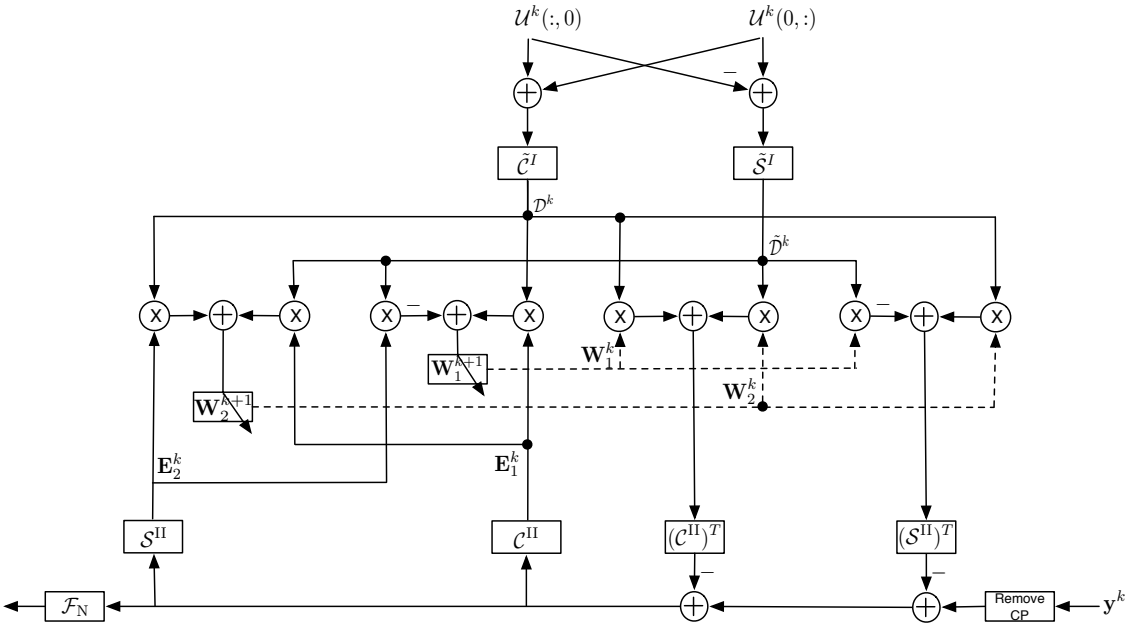

Fig. 2: Block diagram of the unconstrained mixed trigonometric canceller (MTC).

matrix (34) for the CMDC algorithm takes the form

$$\mathcal{R}_{\mathrm{C}} = \mathcal{G}\,\mathcal{G}^H\,\mathrm{E}[(\mathcal{S}^k)^H\,\mathcal{G}\,\mathcal{G}^H\,\mathcal{S}^k]\,\mathcal{G}\,\mathcal{G}^H, \tag{35}$$

where we drop the $1/2$ factor, since it does not affect the ratio of eigenvalues. Since the matrices $\mathcal{G}$ and $\mathcal{G}^H$ are deterministic, they can be moved inside the expectation operation, and (35) can be rewritten as

$$\mathcal{R}_{\mathrm{C}} = \mathcal{G}\,\mathrm{E}[\mathcal{G}^H\,(\mathcal{S}^k)^H\,\mathcal{G}\,\mathcal{G}^H\,\mathcal{S}^k\,\mathcal{G}]\,\mathcal{G}^H = \mathcal{G}\,\mathrm{E}[(\mathcal{U}^k)^T\,\mathcal{U}^k]\,\mathcal{G}^H. \tag{36}$$

It can easily be verified that $\mathcal{R}_{\mathrm{LMS}} = \mathrm{E}[(\mathcal{U}^k)^T\,\mathcal{U}^k]$ is the correlation matrix determining the convergence rate of the time-domain LMS echo canceller.

We know from the above discussion that $\mathcal{R}_{\mathrm{C}}$ has only $2N - l_c = N$ non-zero eigenvalues. In addition, the eigenvalues of $\mathcal{R}_{\mathrm{C}}$ are given by the roots of the following characteristic polynomial: $\det(\lambda\mathcal{I}_{2N} - \mathcal{R}_{\mathrm{C}}) = \det(\lambda\mathcal{I}_{2N} - \mathcal{G}\,\mathcal{R}_{\mathrm{LMS}}\,\mathcal{G}^H)$. Using the formula for the determinant of partitioned matrix in terms of its submatrices [21], it can be easily verified that the N non-zero eigenvalues of $\mathcal{R}_{\mathrm{C}}$ are the same as the eigenvalues of the correlation matrix $\mathcal{R}_{\mathrm{LMS}}$. Therefore, the time-domain LMS echo canceller and the proposed CMDC algorithm have equivalent convergence behaviour, which also agrees with the simulation results presented in Section VII. The unconstrained MDC algorithm has slower convergence rate compared to that of the CMDC as expected, which is discussed in detail in Section VII.

VI. Implementation of Mixed-domain Cancellers

So far, we have developed the general mixed-domain echo canceller structure, referred to as MDC, and its constrained counterpart with the addition of linear constraints, referred to as CMDC. In this section, we examine the implementation of these cancellers and possible performance improvements gained by employing a specific decomposition.

A. Mixed trigonometric canceller

The mixed-domain cancellers can be implemented using different decompositions of the Toeplitz data matrix, which results in different cancellers with varied performance in terms of complexity and convergence rate. Based on the MDC structure, we can determine some intuitive criteria for an *appropriate* decomposition, in the sense of reducing the complexity. As can be seen from (25), for a decomposition where the submatrices $\mathcal{S}_{i,j}^k$ $(i,j = 1,2)$ of $\mathcal{S}^k$ are diagonal or at most tridiagonal, the echo canceller weights can be updated in exact form with low computational complexity. In addition, a decomposition is preferred where the transformations (defined by the submatrices of $\mathcal{G}$) can be implemented efficiently.

The symmetric decomposition defined in (15), which is based on the discrete trigonometric transformations, satisfies both of these conditions. In this decomposition, as discussed in Section III-A, the submatrices of $\mathcal{S}^k$ have non-zero elements only on the main diagonal, on the sub-diagonal or on the super-diagonal. In addition, the required transformations for the decomposition are discrete trigonometric transformers for which efficient algorithms are available [16].

We refer to this realization of the mixed-domain structures using the symmetric decomposition as the mixed trigonometric canceller (MTC). The block diagram for this canceller implementation is given in Fig. 2, where the decomposition of the Toeplitz matrix is done by the DCT-I and DST-I. The estimated echo is calculated in the transform domain and afterwards mapped into the time domain using the inverse DCT-II and inverse DST-II, to be subtracted from the received signal. The error signal is mapped into the transform domain using the DCT-II and DST-II, and the weights are updated based on (25) in the transform domain. It should be noted that the operations of shift by the matrices $\mathcal{Z}$ and $\tilde{\mathcal{Z}}$ and complex conjugation are not shown in the block diagram, for readability.

In the proposed MTC algorithm, we can actually utilize a combination of constrained and unconstrained mixed-domain

TABLE I: Complexity comparison between the combined MTC algorithm and the existing echo cancellers.

Application	Echo Emulation	Adaptive Update	Total
LMS	$T_e\,N$	$T_e\,N$	$2T_e\,N$
CES	$2N+\frac{(T_e-\upsilon-1)^2}{2}$	$N\log_2 N-N+4$	$N\log_2 N+N+\frac{(T_e-\upsilon-1)^2}{2}+4$
CDC	$2N\log_2 N+N+6$	$2N+\frac{1}{\psi}(1.5N\log_2 N-2.5N+6)$	$2N\log_2 N+3N+6$ $+\frac{1}{\psi}(1.5N\log_2 N-2.5N+6)$
SDC	$3N\log_2 N+3N+8$	$2N$	$3N\log_2 N+5N+8$
MTC	$2N\log_2 N+2N+2$	$N\log_2 N+4N+\frac{1}{\phi}(2N\log_2 N)$	$3N\log_2 N+6N+2$ $+\frac{1}{\phi}(2N\log_2 N)$

structures for the adaptive weight update step, incorporating them into a single, yet flexible algorithm. In this *combined* MTC algorithm, the weights are updated by (25) for all iterations k, unless for iterations where k is a multiple of integer $\phi > 0$, where they are updated by (30). In this case, different values of ϕ result in different cancellers. For instance, for $\phi = 1$, the constraint is applied at each iteration, which corresponds to the CMDC; for $\phi = \infty$, no constraint is applied, which corresponds to the MDC and for other values of ϕ, the constraint is applied in each ϕ^{th} interval. As the simulation results in Section VII and the computational complexity analysis in the next section show, the parameter ϕ in the combined MTC algorithm can be used to achieve the desired trade-off between the complexity and convergence behaviour. Therefore, depending on the available resources and the required convergence time, proper value for the parameter ϕ can be chosen. The MTC with $\phi = 1$, corresponding to CMDC, has the highest computational complexity and fastest convergence rate, while the MTC with $\phi = \infty$, corresponding to MDC, has the lowest computational complexity and slowest convergence rate for the family of combined MTC algorithms.

B. Complexity analysis of MTC

The computational complexity of the combined MTC algorithm is compared with that of existing methods in Table I. The comparison is performed for the general case of $T_e \leq N$, and the complexity is expressed as the number of real multiplications at the symbol rate. The decomposition of the matrix $\mathcal{U}^k$ is done by using a $2N$-point FFT based on the method in [22], using the split-radix FFT algorithm. The transformations by the DCT and DST are performed by the radix-2 fast recursive algorithm as in [23].

As it can be seen, the time-domain LMS method requires the largest number of computations and the CES algorithm requires the least; however, the latter is sensitive to lack of excitation on the unused tones. For large frame sizes, the SDC method is more efficient to implement than the CDC scheme. The proposed combined MTC algorithm has approximately the same computational cost as the CDC and SDC methods. However, as it would be shown in Section VII, the combined MTC method convergences faster than the CES and CDC methods and does not suffer from the lack of excitation on the tap-input vector used to update the weights.

The complexity of the digital part of a DMT-based ADSL transceiver (excluding the Reed-Solomon encoder/decoder) is approximately $3N\log_2 N$ [24], [25]. As it can be seen from Table I, the complexity of the echo canceller which is of order $O(N\log_2 N)$ is comparable to the complexity of the ADSL transceiver. Consequently the performance improvements achievable by using echo canceller in comparison to a FDD system, as discussed in Section I, are attainable if the additional increase in the complexity can be tolerated.

VII. Simulation Results

In this section, we use simulation experiments to evaluate the convergence behaviour of the proposed mixed-domain echo canceller and the existing echo cancellers. In the simulations, an ADSL system over the carrier serving area (CSA) loop #4 is used [1]. DMT modulation is employed where tones 7-31 and 33-255 are allocated for the upstream and downstream, respectively and each tone transmits a 4-QAM signal constellation. The downstream and upstream signal transmit with -40 dBm/Hz, and the external additive noise is white Gaussian noise at -140 dBm/Hz. The transmit block length in the upstream and downstream is 64 and 512, respectively and the corresponding cyclic prefix length is 5 and 40, respectively. The true echo channel contains 512 samples at sampling rate of 2.2MHz, including the effect of the hybrid[5], the transmitter and receiver filters and the time-domain equalizer (TEQ). The front-end receiver filter and the filter involved in DAC are modeled as Butterworth lowpass filters with corner frequencies of 1.104 MHz and 138 kHz, respectively. The TEQ coefficients are calculated using the MATLAB Toolbox developed in [28], using MMSE Unit Tap Constraint method. For the adaptive cancellers, the

[5]For additional details on the implementation and parameters of active-RC type hybrid networks, the reader may consult the following sources: [26] and [27].

TABLE II: Simulated eigenvalue spread for different echo cancellation algorithms.

LMS EC	CES EC	CDC	MTC $\phi = \infty$	MTC $\phi = 1$
3.2	11.9	14.8	15.7	3.2

echo channel weight vectors are initialized to all-zero, and no data is sent on the unused tones. It should be noted that for these multirate simulations, the proposed algorithms are extended using the methods discussed in [9] for multirate echo cancellers.

In connection to the discussion on the convergence rate using the eigenvalue spread of the correlation matrix during the adaptation in Section V, we calculated the eigenvalue spread using computer simulations, where the results for different echo cancellation algorithms are given in Table II. These results are obtained by assuming a symmetric rate at the transmitter and the receiver, equal length of the echo channel with the frame size and excitation on all tones[6]. As it can be seen, the time-domain LMS echo canceller and MTC algorithm with $\phi = 1$ (realizing CMDC) have the same eigenvalue spread which is in compliance with the discussion in Section V. Comparing the results for the MTC with $\phi = \infty$ (realizing MDC), CES and CDC algorithms, at first it may seem that the CES and CDC algorithms have faster convergence compared with that of the unconstrained MTC method. However, these results do not reflect the effect of the insufficient excitation caused by unused tones in the frequency domain and also the error cause by approximate weight update in the frequency domain which is used in the CES and CDC algorithms. In practice, these factors deteriorate the performance of the CES and CDC algorithms and a better comparisons of the convergence rate of these algorithms is performed by simulating their learning curves which are discussed below. The performance index is the mean squared error (MSE) of the residual echo.

We first consider a case, where the length of the echo canceller weight vector is assumed to be equal to the frame size, i.e., $T_e = 512$. It should be noted that the SDC algorithm is presented only for symmetric rate implementations in [11], where in this work in order to make the comparisons with other methods possible, we extended this algorithm so that it can be implemented at the RT receiver using interpolated input data matrix. The learning curves for the frame synchronous system at the RT receivers are depicted in Fig. 3 and Fig. 4[7]. In Fig. 3, the step-size parameter μ is chosen to ensure that the cancellers have a similar error floor, and in Fig. 4, the step-size parameter is chosen to ensure that the cancellers have similar initial convergence slope. For the MTC algorithm used in this case $\phi = 1$ corresponding to the CMDC algorithm.

The results in Fig. 3 and Fig. 4 show that the time-domain LMS canceller and the constrained MTC method have similar

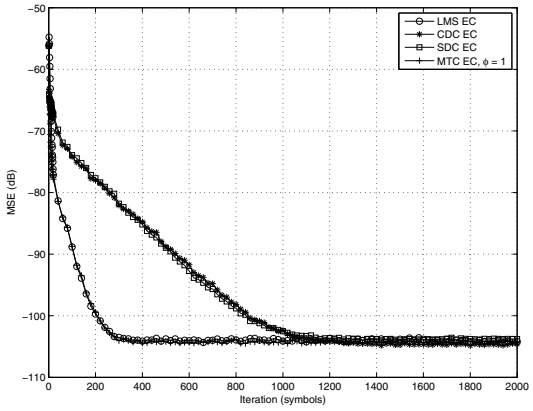

Fig. 3: Convergence behaviour of different echo cancellation methods for synchronous ADSL-RT, $T_e = 512$

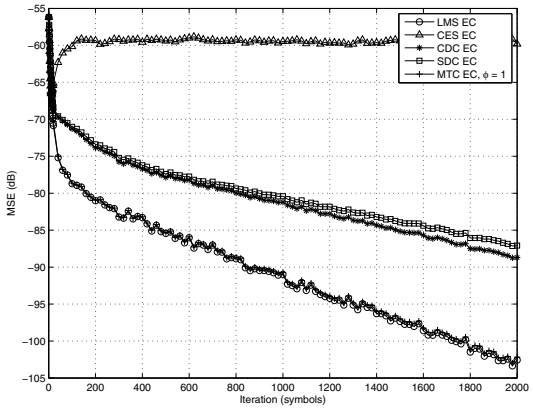

Fig. 4: Convergence behaviour of different echo cancellation methods for synchronous ADSL-RT, $T_e = 512$

performance and have faster convergence compared with the CDC, SDC and CES algorithms. As discussed in [11], the SDC method has a similar convergence rate to the CDC algorithm. For the CES algorithm in the case of $T_e = 512$, the canceller diverges after an initial convergence because of the error accumulation in the tail weights. In Fig. 5, similar comparisons are presented for the CO receiver, where the results follow the same trend as above.

In the second set of simulations, the convergence rate of the combined MTC algorithm for different values of ϕ is examined. The simulations results for the above scenario at the RT and CO receivers are depicted in Fig. 6 and Fig. 7, respectively. It can be seen that for both receivers, the unconstrained algorithm ($\phi = \infty$) has the slowest convergence rate, as expected, and the constrained one ($\phi = 1$) has the fastest because of the reduced degrees of freedom. However, the combined MTC algorithms with $\phi = 10$ and 50 achieve a close performance to that of the constrained MTC algorithm, which shows that the loss of convergence speed by using the infrequent constrained update is small.

In the third set of simulations, the performance of the

[6]The system condition of having excitation on all tones is only used for the results in Table II.

[7]More efficient implementations of the multi-rate MTC algorithm is discussed in [29]

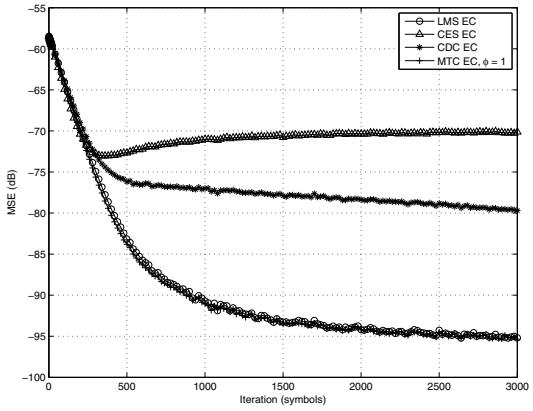

Fig. 5: Convergence behaviour of different echo cancellation methods for synchronous ADSL-CO, $T_e = 512$

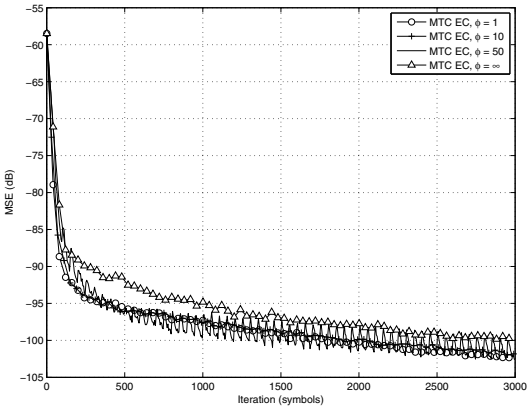

Fig. 7: Convergence behaviour of Combined MTC algorithm with different intervals of application of the constraint gradient for synchronous ADSL-CO, $T_e = 260$

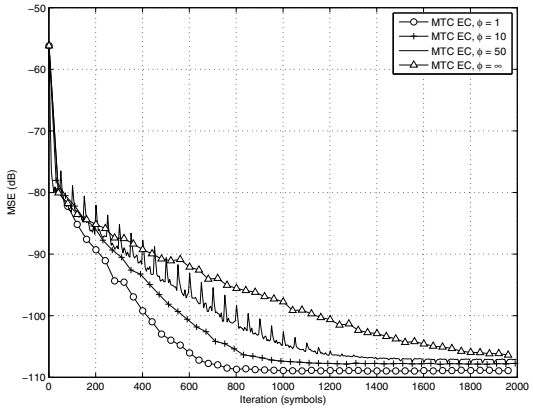

Fig. 6: Convergence behaviour of Combined MTC algorithm with different intervals of application of the constraint gradient for synchronous ADSL-RT, $T_e = 260$

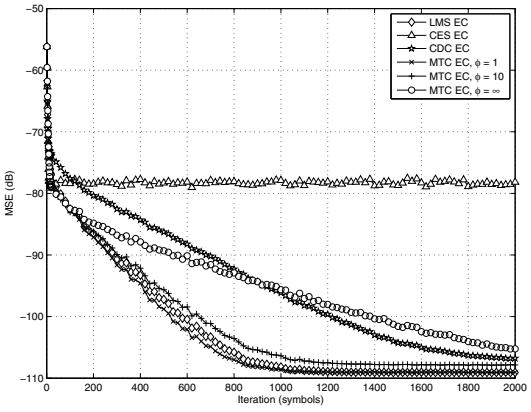

Fig. 8: Convergence behaviour of different echo cancellation methods for synchronous ADSL-RT, $T_e = 260$

combined MTC algorithm is compared with those of the existing echo cancellers, for the case where the length of the echo canceller is shorter than the frame size, i.e., $T_e = 260$[8]. The learning curves for the frame synchronous system at the RT and CO receivers, are depicted in Fig. 8 and Fig. 9, respectively. For the combined MTC algorithm, different time intervals for applying the gradient constraint are examined, i.e., $\phi = 1, 10, \infty$. As seen in Fig. 8 and Fig. 9, the MTC method with no gradient constraint ($\phi = \infty$) performs better than the CDC and CES algorithms. In addition, the combined MTC method with $\phi = 1$ performs equivalent to the time-domain LMS canceller, and the MTC with $\phi = 10$ provides a very close convergence to these two algorithms with reduced computational complexity.

We note that for the case of $T_e < N$, the convergence is always faster than in the case of $T_e = N$, since the last $N - T_e$ weights are forced to zero. That is, the number of adaptive degrees of freedom has been reduced. This improvement can be clearly seen by comparing the results for ADSL-RT in Fig. 4 and Fig. 8, and for ADSL-CO in Fig. 5 and Fig. 9. Therefore, the theoretical convergence analysis for the case $T_e = N$ can be seen as a lower bound on the convergence rates for $T_e < N$.

In practice, the residual echo (MSE) at the decoder can be considered as a distortion that is added to the background noise. Therefore, reducing the residual echo would result in a higher operating SNR which translates into lower BER, where these performance measures are also affected by the utilized modulation and coding schemes. In case the background noise is dominated by other sources, e.g., the crosstalk, their presence could be reflected by increasing the noise floor. It is also important to note that the provided results are not dependent on the specific CSA test loop chosen, similar experiments on other test loops reached similar conclusions as those reported in this paper (i.e., similar behaviour in terms of convergence rate and residual MSE).

[8]It should be noted that the SDC algorithm is not simulated for this scenario, since it is developed only for $T_e = N$ in [11].

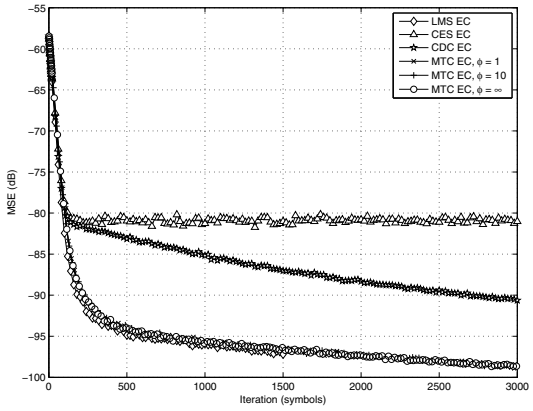

Fig. 9: Convergence behaviour of different echo cancellation methods for synchronous ADSL-CO, $T_e = 260$

VIII. Conclusion

In this paper, we studied the mixed-domain echo cancellation for DMT-based system, in detail. We presented a general decomposition for the Toeplitz data matrix and shown that it provides a uniform description of the decompositions used in the existing echo cancellers. Based on this general form, a new mixed-domain canceller (MDC) was proposed, where the exact LMS-type adaptive weight update is performed in the transform domain. Later, we presented the linear constrained mixed-domain cancellers (CMDC), where additional constraints can be added to the system to improve its performance. We also showed that for these mixed-domain configurations, an appropriate decomposition is the symmetric decomposition, which results in an implementation referred to as mixed trigonometric canceller (MTC). We also proposed a combined MTC algorithm which was shown to have a faster convergence rate than existing cancellers with the similar computational complexity. This structure is also robust against the lack of excitation on the unused tones and does not require the transmission of dummy data therefore.

References

[1] T. Starr, J. M. Cioffi, and P. J. Silverman, *Understanding Digital Subscriber Line Technology*. Prentice Hall, 1999.

[2] F. Sjoberg, M. Isaksson, R. Nilsson, P. Odling, S. K. Wilson, and P. O. Borjesson, "Zipper: a duplex method for VDSL based on DMT," *IEEE Trans. Commun.*, vol. 47, no. 8, pp. 1245–1252, Aug. 1999.

[3] D. Mestdagh, M. R. Isaksson, and P. Odling, "Zipper VDSL: a solution for robust duplex communication over telephone lines," *IEEE Commun. Mag.*, vol. 38, no. 5, pp. 90–96, May 2000.

[4] S. Wilmoesterer (2005, July), Future proof telecommunications networks with VDSL2. VDSL2_WP_072005_v1.1_1.pdf. Available: http://www.infineon.com/

[5] S. Haykin, *Adaptive Filter Theory*, 4th edition. Prentice Hall, 2001.

[6] D. Mestdagh, P. Spruyt, B. Biran, and H. Verbueken, "Echo cancellation versus FDM for DMT-based ADSL: a comparative study of system performance and implementation complexity," *Amer. Nat. Stand. Inst., Tech. Rep. T1E1*, vol. 4, pp. 93–131, 1993.

[7] "Very high speed digital subscriber line transceivers 2 (VDSL2)," ITU-T Recommendation G.993.2, Feb. 2006.

[8] J. M. Cioffi and J. A. C. Bingham, "A data-driven multitone echo canceller," *IEEE Trans. Commun.*, vol. 42, no. 10, pp. 2853–2868, Oct. 1994.

[9] M. Ho, J. M. Cioffi, and J. A. C. Bingham, "Discrete multitone echo cancelation," *IEEE Trans. Commun.*, vol. 44, no. 7, pp. 817–825, July 1996.

[10] G. Ysebaert, F. Pisoni, M. Bonaventura, R. Hug, and M. Moonen, "Echo cancellation in DMT-receivers: circulant decomposition canceler," *IEEE Trans. Signal Process.*, vol. 52, no. 9, pp. 2612–2624, Sep. 2004.

[11] F. Pisoni and M. Bonaventura, "A multi-carrier echo canceller based on symmetric decomposition," in *Proc. 2005 IEEE Workshop Signal Process. Syst. Design Implementation*, pp. 233–238.

[12] M. Ho, "Multicarrier echo cancellation and multichannel equalization," Ph.D. dissertation, Dept. Elect. Eng., Stanford University, CA, 1995.

[13] G. Ysebaert, "Equalization and echo cancellation for DMT-based systems," Ph.D. dissertation, Katholieke Universiteit Leuven, Belgium, 2001.

[14] N. Ehtiati and B. Champagne, "Constrained adaptive echo cancellation for discrete multitone systems," *IEEE Trans. Signal Process.*, vol. 57, no. 1, pp. 302–312, Jan. 2009.

[15] D. Potts and G. Steidl, "Optimal trigonometric preconditioners for nonsymmetric Toeplitz systems," *Linear Algebra Appl.*, vol. 281, pp. 265–292, 1998.

[16] V. Britanak, P. C. Yip, and K. R. Rao, *Discrete Cosine and Sine Transforms: General Properties, Fast Algorithms and Integer Approximations*. Academic Press Inc., 2006.

[17] N. Ehtiati and B. Champagne, "Dual transform domain echo canceller for discrete multitone systems," in *Proc. IEEE Globecom*, pp. 3032–3037.

[18] ——, "Comparative evaluation of the dual transform domain echo canceller for DMT-based systems," in *Proc. 2010 IEEE International Conf. on Acoustics Speech and Signal Processing*, pp. 3318–3321.

[19] O. L. Frost, "An algorithm for linearly constrained adaptive array processing," *Proc. IEEE*, vol. 60, no. 8, pp. 926–935, Aug. 1972.

[20] L. Griffiths and C. Jim, "An alternative approach to linearly constrained adaptive beamforming," *IEEE Trans. Antennas Propag.*, vol. 30, no. 1, pp. 27–34, Jan. 1982.

[21] G. H. Golub and C. F. Van Loan, *Matrix Computations*, 3rd edition. Johns Hopkins University Press, 1996.

[22] H. Guo, G. Sitton, and C. Burrus, "The quick Fourier transform: an FFT based on symmetries," *IEEE Trans. Signal Process.*, vol. 46, no. 2, pp. 335–341, Feb. 1998.

[23] P. Z. Lee and F.-Y. Huang, "Restructured recursive DCT and DST algorithms," *IEEE Trans. Signal Process.*, vol. 42, no. 7, pp. 1600–1609, July 1994.

[24] B. Shim and N. Shanbhag, "Complexity analysis of multicarrier and single-carrier systems for very high-speed digital subscriber line," *IEEE Trans. Signal Process.*, vol. 51, no. 1, pp. 282–292, 2003.

[25] B. Wiese and J. S.Chow, "Programmable implementations of xDSL transceiver systems," *IEEE Commun. Mag.*, vol. 38, no. 5, pp. 114–119, 2000.

[26] W. Y. Chen, J. L. Dixon, and D. L. Waring, "High bit rate digital subscriber line echo cancellation," *IEEE J. Sel. Areas Commun.*, vol. 9, no. 6, pp. 848–860, Aug. 1991.

[27] W. Y. Chen, *DSL: Simulation Techniques and Standards Development for Digital Subscriber Line Systems*. Macmillan Technical Publishing, 1998.

[28] G. Arslan and B. Lu (2003, May), "Time domain equalizer design for discrete multitone modulation. dmtteq3_1.zip. Available: http://users.ece.utexas.edu/~bevans/projects/adsl/dmtteq/dmtteq.html

[29] N. Ehtiati and B. Champagne, "Dual domain echo cancellers for multirate discrete multitone systems," in *Proc. 2010 Asilomar Conf. Signals, Syst. Comput.*

Neda Ehtiati received the B.S. degree from University of Tehran, Iran, in 2001, the M.S. degree from Concordia University, Montreal, Canada, in 2004 and the Ph.D. degree from McGill University, Montreal, Canada, in 2011, all in Electrical Engineering. She is currently working as an algorithm specialist at Octasic Semiconductor Inc., where she is responsible for designing advanced signal processing algorithms for various applications such as speech processing and communication systems, optimized for multi-core DSP processors. Her research interests are in the area of signal processing and information theory for communication systems, including echo cancellation, speech enhancement and coding techniques.

Benoît Champagne received the B.Ing. degree in Engineering Physics from the Ecole Polytechnique de Montral in 1983, the M.Sc. degree in Physics from the Universit de Montral in 1985, and the Ph.D. degree in Electrical Engineering from the University of Toronto in 1990. From 1990 to 1999, he was an Assistant and then Associate Professor at INRS-Telecommunications, Universit du Quebec, Montral. In 1999, he joined McGill University, Montreal, where he is now a Full Professor within the Department of Electrical and Computer Engineering. He also served as Associate Chairman of Graduate Studies in the Department from 2004 to 2007.

His research focuses on the development and performance analysis of advanced algorithms for the processing of information bearing signals by digital means. His interests span many areas of statistical signal processing, including detection and estimation, sensor array processing, adaptive filtering, and applications thereof to broadband communications and speech processing, where he has published extensively. His research has been funded by the Natural Sciences and Engineering Research Council (NSERC) of Canada, the "Fonds de Recherche sur la Nature et les Technologies" from the Government of Quebec, Prompt Quebec, as well as some major industrial sponsors, including Nortel Networks, Bell Canada, InterDigital and Microsemi.

He has been an Associate Editor for the IEEE Signal Processing Letters and the *EURASIP Journal on Applied Signal Processing*, and has served on the Technical Committees of several international conferences in the fields of communications and signal processing. His is currently an Associate Editor for the IEEE TRANSACTIONS ON SIGNAL PROCESSING and a Senior Member of IEEE.